Automated modal parameter tracking with neural network based normalization of environmental perturbations

Johann Priou, Szymon Gres, Matthieu Perrault, Laurent Guerineau, Mathieu Desbazeille, Michael Döhler

EWSHM 2024
11th European Workshop on Structural Health Monitoring

Automated modal parameter tracking with neural network based normalization of environmental perturbations

Johann PRIOU[1], Szymon GREŚ[2], Matthieu PERRAULT[3], Laurent GUERINEAU[3], Mathieu DESBAZEILLE[3], and Michael DÖHLER[1]

[1] Univ. Gustave Eiffel, Inria, COSYS/SII, I4S, Rennes, France, michael.doehler@inria.fr
[2] Aarhus University, Dept. of Civil and Architectural Engineering, Aarhus, Denmark
[3] Sercel, Carquefou, France

Abstract. Automated modal parameter tracking is an essential part of vibration-based structural health monitoring of engineering structures, e.g., bridges, high-rise buildings, wind turbines, amongst others. In this work, we conceive a robust algorithm for accomplishing this task. First, the modal parameters are extracted by greedy clustering the stabilization diagram, which is based on covariance-driven subspace identification and the related uncertainty quantification. After the selection of a set of relevant modal parameters to be monitored, the tracking is performed by an active search of stable modes close to the reference ones with using statistical criteria and automated clustering. The applied strategies depict a tracking approach that is robust to relatively strong variations in the natural frequencies, or the MAC, without losing track of the monitored modes. Finally, when environmental and operational variables (EOVs) are measured and training and testing periods are defined, a neural network is trained based on the tracked frequencies and the EOVs, with the goal of correcting the environmental influence on the estimated frequencies based on the model predictions. In doing so, a distance metric is defined for damage detection, which is robust to environmental perturbations under the measured EOVs. The whole framework is showcased on monitoring data of a full-scale bridge.

Keywords: Operational modal analysis · uncertainty quantification · stabilization diagram · automated interpretation · greedy clustering · subspace methods · neural network

1 Introduction

Automated damage detection in the context of vibration-based structural health monitoring (SHM) system can be divided into three parts: data acquisition, extraction of damage-sensitive features, and eventually statistical analysis of these features [1]. Therein, the removal of environmental and operational effects (EOVs) plays a key role in the appliance of SHM concept to engineering systems in-operation. Modal parameters are used as damage-sensitive features from the dawn of the SHM field. Under ambient excitation conditions, the collected data contains information on both the structural modes, but also on dynamic disturbances due to colored excitation and measurement noise. This poses a challenge for the automated identification of the modal parameters and motivates the use of engineering tools like stabilization diagrams to accomplish this task. Over the last decade, extensive research has been devoted to developing automated strategies to extract the physical modes from stabilization diagrams [2,3], usually based on different distance metrics between the modes and clustering strategies. The drawback of classical clustering approaches is that usually either the number of clusters, i.e., the number of modes, or thresholds on distance measures need to be set by the user.

Media and Publishing Partner

In this work, an efficient greedy strategy for automated interpretation of stabilization diagrams is used [4], where intrinsic thresholds based on the statistical uncertainty bounds of the modal parameters [5,6,7] are used instead of user-defined thresholds, together with an associated algorithm for modal tracking under possibly strong variations [4].

Changes in temperature, traffic loads, and wind loads often cause a more significant shift in modal parameters than local structural damages. Therefore, it is imperative to identify these confounding effects and to remove them from the features before diagnosing damages. Various methods exist for such a data normalization and they are commonly categorized based on whether the EOVs are measured or not. When EOVs are not measured, common methods involve linear principal component analysis (PCA) [8], second-order blind identification (SOBI) [9], and kernel PCA [10]. Yet, the interpretation of results and the hyper-parameter tuning can be challenging. On the other hand, the method class using the measured EOVs comprises linear regression [11], neural networks [12], or Gaussian Process models [13], to name a few.

In this article, a simple neural network-based data normalization is applied to remove the effect of EOVs, followed by an anomaly detection by means of the Mahalanobis distance. The benefits of the presented approach is the robustness of its automated modal parameter identification towards noise as well as towards possibly strong changes during tracking, without the requirement of individual parameter tuning. The application of the proposed framework is illustrated on long-term monitoring data of a pedestrian bridge in Grenoble (France) and evaluated towards diverse EOV settings.

2 Modal parameter tracking and normalization

In this section we outline the methods used for automated modal parameter estimation and tracking, data normalization and robust change detection.

2.1 Modal parameter estimation

The natural frequencies, damping ratios, and mode shapes are obtained with the reference-based covariance-driven subspace algorithm at multiple model orders [14,15] for their evaluation in stabilization diagrams. Furthermore, the associated uncertainty quantification [5,6,16] is carried out to obtain the uncertainty bounds of each of the modal parameter estimates. In a preliminary step, the uncertainties are used to remove modes with high uncertainty from the stabilization diagram, as they are likely to be noise modes. The threshold for the removal should not be too strict, and can be set for the frequency coefficient of variation at, e.g., 5%. The computed uncertainty bounds will then play a crucial role in the automated interpretation of the stabilization diagram, since they offer intrinsic thresholds for clustering the modes, as presented in [4].

For this task, non-physical estimates are cleared and physical modal parameter estimates are aggregated in modal alignments based on statistical inference. In a computationally efficient greedy strategy modal alignments with the largest number of statistically compliant modal parameter estimates are obtained, one after another, beginning with an estimate in a high modal density region in the diagram. To further increase robustness of the approach, a post-processing step checks if the obtained alignments are too strictly or too loosely chosen. In the first case, a merging step takes care of close neighbors, and in the second case a separation step removes possibly redundant and spurious modes from the alignment.

Finally, alignments are checked again for their statistical coherence, and the global modal parameter estimates are developed as a weighted average from the alignment, where the weights

are proportional to their statistical uncertainty. As a result, the more uncertain modal estimates are penalized and the resultant covariance of the weighted mean appears to be lower than the mean covariance of the underlying parameter estimates [17].

2.2 Modal parameter tracking

First, a set of reference modes is obtained from the chosen reference data set(s). Then the reference modes are searched for in any new dataset that is analyzed, based on the following steps:

- Basket creation: A "basket" in the vicinity of the tracked mode is created directly in the analyzed stabilization diagram, without clustering. If the tracked mode is not present (e.g., due to low excitation), the modal analysis is repeated at higher model orders.
- Clustering: The method from the previous section provides alignments in each of the baskets. If more than one alignment is found, then the closest to the reference mode is kept. The global modal parameters are computed from the alignment.
- Update: It is suggested to use an evolving set of reference modes, where a part of them is updated with the newly found modes.

2.3 Data normalization

Neural networks can be used to model the relationship between EOVs and the natural frequencies. It is supposed that training data $\{(T^j, f_i^j)\}$, $j = 1, \ldots, n_d$, is available from n_d datasets in the reference state, which reflects the relation between the EOV vector T and each frequency $i = 1, \ldots, n_m$, where n_m is the number of modes. From the training data a model $\tilde{f}_i = g_i(T)$ is learned describing this relationship, and then applied to new, incoming data for data normalization. For data normalization, a reference value of the EOV T^{ref} is defined, to which the normalized frequencies will correspond to, and let $f_i^{\text{ref}} = g_i(T^{\text{ref}})$. Then, the normalization of a new measurement (T^*, f_i^*) can be carried out as described in [18] by:

$$\check{f}_i^* = \frac{f_i^*}{g_i(T^*)} f_i^{\text{ref}}. \tag{1}$$

2.4 Change detection

Change detection is made with Mahalanobis distance which describes a distance between a reference dataset and a frequency or a vector of frequencies f computed as

$$D_m^c = \sqrt{(f - \mu_{f^{ref}})^T \Sigma_{f^{ref}}^{-1} (f - \mu_{f^{ref}})} \tag{2}$$

where $\mu_{f^{ref}}$ and $\Sigma_{f^{ref}}$ are sample mean and covariance computed from a reference dataset. This distance can be computed on a single mode, or combined on all modes. The distribution of the squared Mahalanobis distance can be approximated by a χ^2 distribution, and a threshold to distinguish data in the reference state defined for a desired false alarm rate, e.g., 5%.

3 Case study: pedestrian bridge in Grenoble

3.1 Description

Saint-Laurent footbridge is located in Grenoble (France). It is a suspension bridge with cable stays over the Isère river (Figure 1), composed of three spans: one central suspended span of

length 62m with a deck made of steel and concrete, and two lateral masonry 10m-spans. The structure has a total length of 82m and a total width of 8m.

The footbridge has been instrumented with the Sercel S-Morpho system within the scope of a research program with La Région Auvergne-Rhône-Alpes. Twelve measurement nodes composed of three-axial accelerometers were installed on the steel part of the main deck with magnets (Figure 1), and their locations are shown in Figure 2. A weather station was also installed at the top of one of the masonry pillar. The structure was continuously monitored from May 2021 to December 2022. In this work, we focus on data from January and February 2022, where acceleration and ambient temperature data were recorded for 20 minutes every hour in 1,414 datasets under ambient excitation.

A preliminary analysis shows that the first six modes of the structure are located within [0-4] Hz. The identified frequencies and damping ratios are shown in Table 1 and the corresponding mode shapes in Figure 3. Modes 1, 2, 5 and 6 are the first four vertical bending modes. Modes 3 and 4 are coupled modes between the first transversal bending mode and the first torsional mode. This coupling may be the effect of the cable stays.

Fig. 1. General view and a measurement node of the Saint-Laurent footbridge.

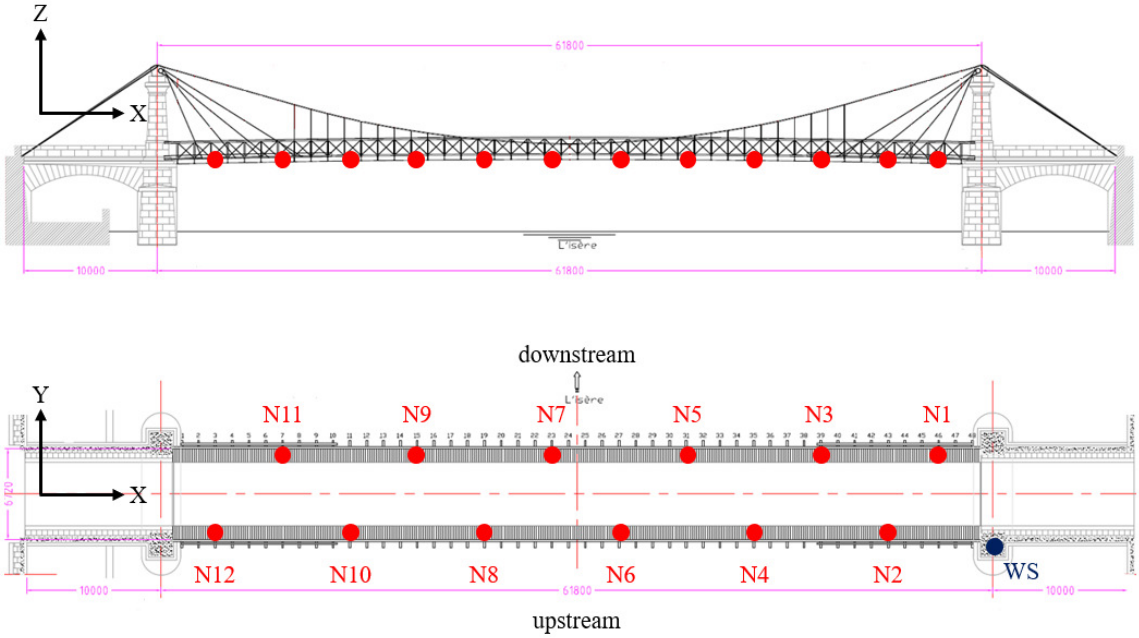

Fig. 2. S-Morpho nodes location on the Saint-Laurent footbridge.

Table 1. Modal parameter estimates from the first examined dataset (V: vertical; T: torsion; L: lateral).

	V1	V2	T1/L1	T1/L1*	V3	V4
Frequency (Hz)	1.39	1.73	2.21	2.60	2.99	3.93
Damping (%)	0.60	1.52	1.38	0.92	0.96	1.54

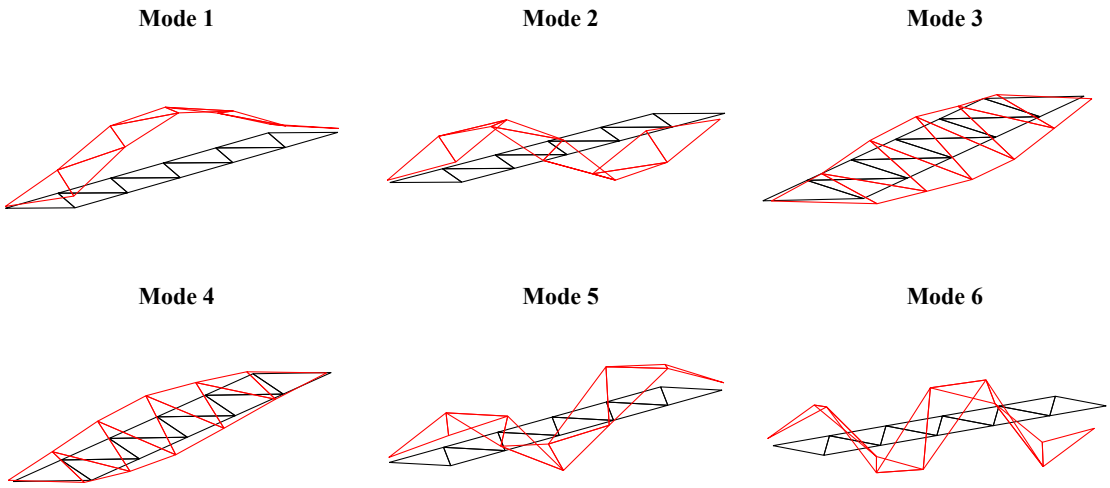

Fig. 3. Mode shapes of the first six modes.

3.2 Modal parameter tracking

After defining the above 6 modes as reference modes, the tracking algorithm is applied on all datasets with results shown in Figure 4. Tracking was successful for more than 99.5% of the modes. All the missed identifications (42 of a total of 8484) were from data during night time between 1 am to 5 am under very low excitation. The tracking results also show a few outliers. A further analysis of these outliers showed that they particularly appear when the structure is subjected to a very high excitation, but the reason for the change in those modes could not be completely determined.

For data normalization the confounding factors need to be determined. The measured temperature seems to be an obvious choice. Due to the mass of the bridge changing with an increased

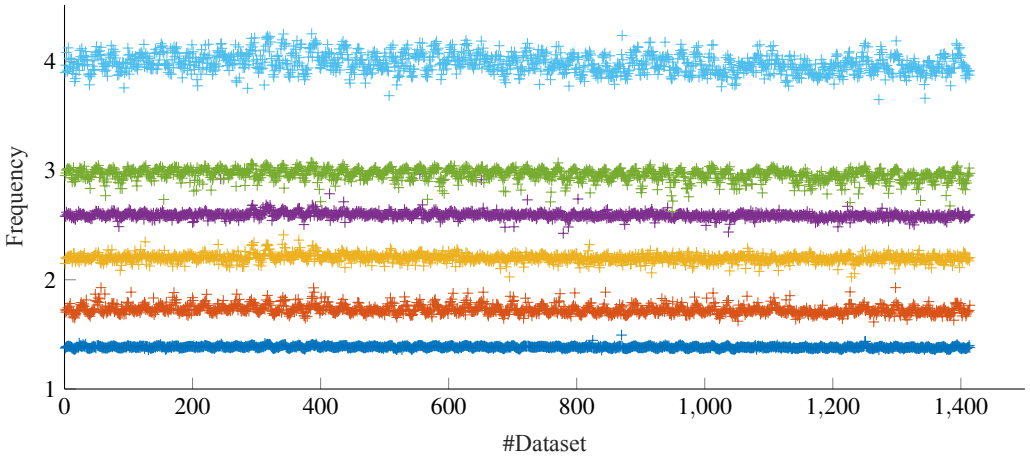

Fig. 4. Tracking of the first 6 modes of the Saint-Laurent footbridge in 1414 datasets over two months.

number of people using the bridge, we propose to use the energy of the acceleration signals in the vertical direction within the typical frequency band of walking or running between 1 and 5 Hz [19] as a proxy for it, since the energy will increase when more people are using the bridge. Figure 5 illustrates the evolution of the first frequency along with the temperature and the energy for some of the datasets. Both EOVs show a daily variation, and correlation with both energy and temperature is visible. Furthermore, Figure 6 details the relation between the energy and the frequency in the frequency histogram of the first mode, where the frequencies estimated from signals with the lowest energies among all datasets are the highest, and the frequencies estimated under the highest energies are the lowest. It is coherent with the pedestrian loading that can excite the structure at a close frequency, and corresponding to acceleration signals with higher energy. Moreover, the mass of a group of people passing by the footbridge could be non negligible and may reduce the natural frequency.

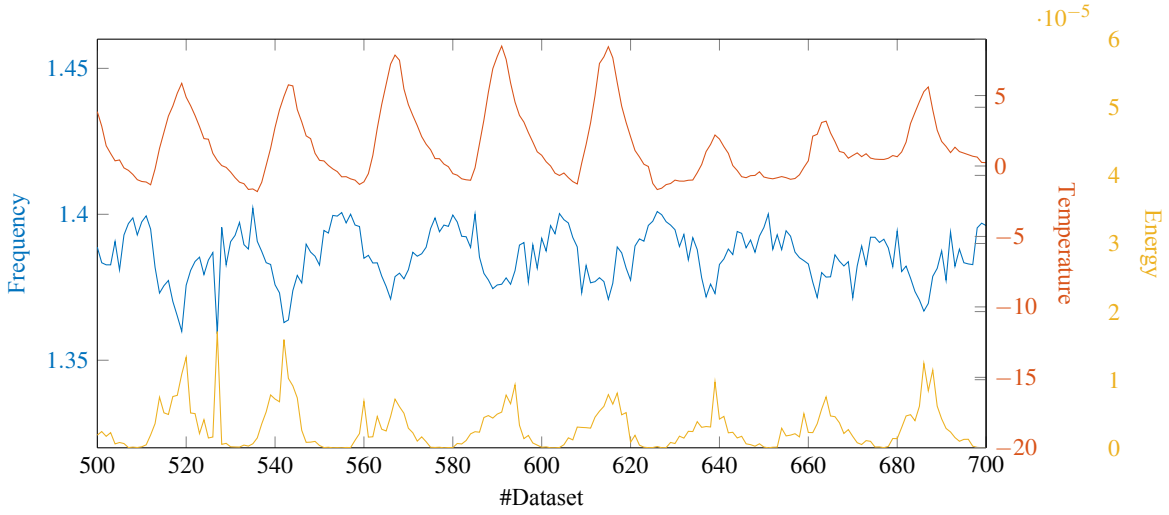

Fig. 5. Evolution of the first frequency, together with temperature and the median of the acceleration signal energy in vertical direction.

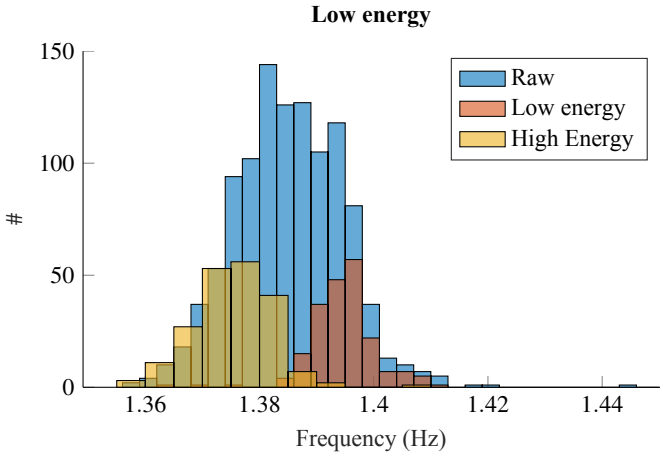

Fig. 6. Histograms of the first natural frequency from all datasets (blue), datasets with lowest energy (orange) and datasets with highest energy (yellow).

3.3 Data normalization

Based on half of the available datasets, neural networks for each frequency are trained with different EOVs as inputs, and then used to normalize the frequencies of the remaining datasets with Eq. (1) for validation. In the training, outliers in the training data have been removed. The performance of the data normalization is evaluated by the sample standard deviations of the normalized frequencies with respect to the original ones. The following EOVs are considered:

- Temperature of the current dataset;
- Temperature of the current and past datasets;
- Energy of the signal;

For a combination of each EOV, the performance on the training data is shown in Figure 7, for each of the modes. It can be seen that the consideration of the temperature history yields better performance than considering the temperature of the current dataset only, possibly due to thermal inertia of the structure. Combining the temperature and the energy yields the highest reduction of uncertainty in the normalized frequencies; however, one can observe that then the consideration of the temperature history seems to be counterproductive for the first modes, or does not yield further reduction of uncertainty in the last modes. It is indeed possible that the effect of the added mass on the structure (visible through the energy) has a more important effect on the frequencies than the thermal inertia (visible through the temperature history).

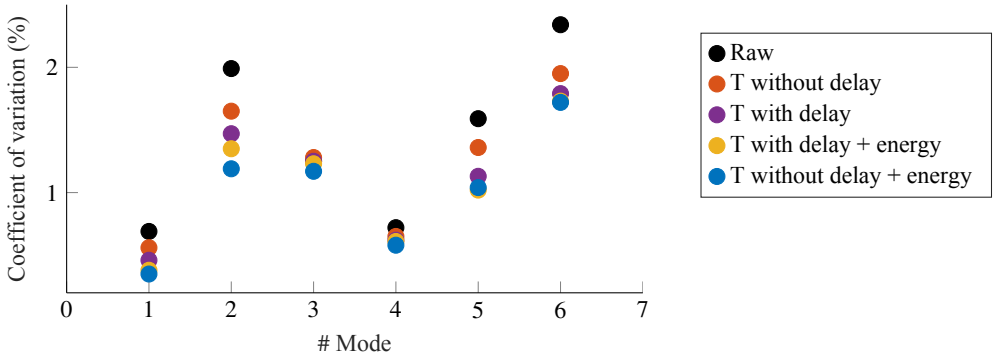

Fig. 7. Coefficient of variation (sample standard deviation divided by the frequency mean) of the normalized frequencies considering different cases of EOVs.

A detailed view on the normalization results for modes 1 and 4 is given in Figure 8 based on the optimized neural network using the current temperature measurement and the energy as EOVs. It can be seen that the first frequency is quite well approximated, only with some difficulties to reach both high and low frequencies in the predictions. The data normalization reduced the sample standard deviation by 50%. The fourth frequency seems to be more complex to approximate, and the standard deviation of the normalized data is not as much reduced, but still shows a reduction by 20%.

Finally, the effect of outliers in the model learning are shown. In the above results, outliers have been cleaned for the training. Note that the validation data has not been cleaned for outliers. Figure 9 shows the frequencies of mode 1 and mode 4 with outliers in red. Mode 1 has the lowest rate of outliers, being at 0.5% of the values. If they are not removed from the training data, then an increase of 11% of the coefficient of variation of the normalized validation data could be observed. Mode 4 is the mode with the highest rate of outliers of around 4%. When they are not

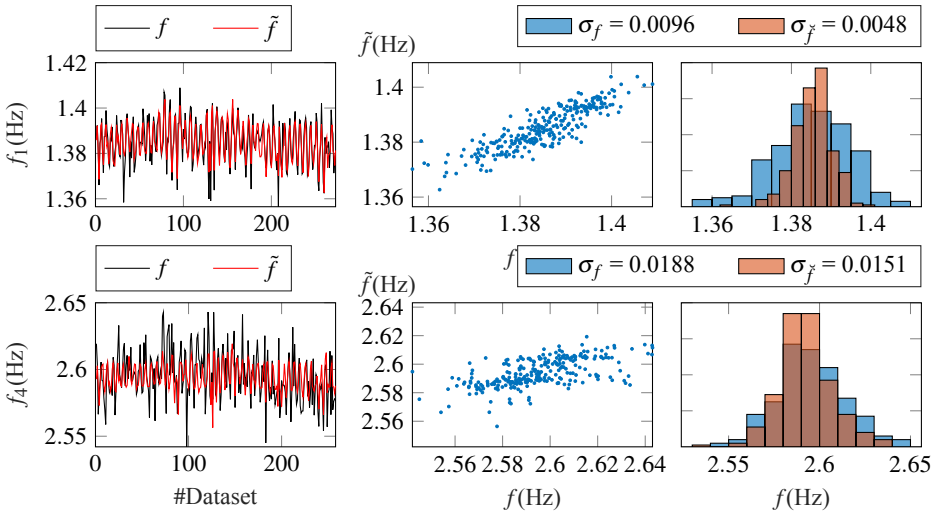

Fig. 8. Left: Estimated natural frequencies f from data (black) and predicted frequencies $\tilde{f}$ from neural network (red). Center: frequency estimate f from the data vs the model output $\tilde{f}$, illustrating the efficiency of the learned model. Right: histogram of estimated frequencies f (blue) and normalized frequencies $\check{f}$ (orange). The top row shows the results for the first frequency, the bottom row for the fourth frequency.

removed in the training, an increase of 130% of the coefficient of variation could be observed. This shows the importance of good training data for a precise consideration of the EOVs.

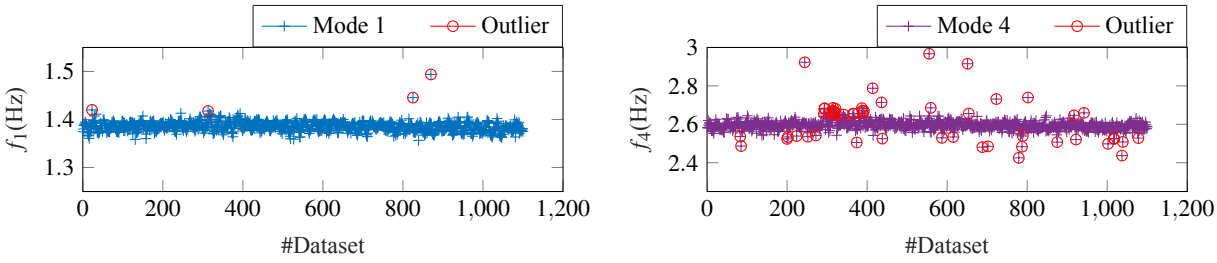

Fig. 9. Frequencies of modes 1 and 4 with outliers showed in red.

3.4 Change detection

In this section, the testing data (comprising half of the available data) is divided into two sets, one to define the distribution properties (i.e., the sample covariance) and the threshold of the Mahalanobis distance (see Section 2.4), and another one for validation. The validation data comprises the frequencies estimated from the last 300 datasets. The threshold to determine the healthy state is defined allowing a 5% false alarm rate for each of the frequencies separately, as well as for the combined evaluation of all six frequencies. Since no data from damaged states is available, the main purpose of this part of the study is to verify if the Mahalanobis distance and the threshold are well-defined for testing purposes, i.e., if the false alarm rate on the testing data remains under the envisaged 5%. It should be noted that the false alarm rate is set quite high in this study for purely academic reasons, namely to verify the distribution properties which requires a sufficient number of samples beyond the threshold while only a limited number of datasets is available. In practice, a lower false alarm rate should be chosen.

To evaluate the importance of the data normalization, we compare the false alarm rates obtained in two setups: first, the frequencies without data normalization are used to define the sample covariance for the Mahalanobis distance, the thresholds, and the testing data; second, these quantities are obtained after data normalization.

In Figure 10 the false alarm rates are shown for the cases without (left) and with (right) data normalization. Using directly the estimated frequencies without normalization (left), two of the modes exceed the threshold and, in particular, the combined evaluation of the six frequencies yields a false alarm rate of more than 10%, more then twice the prescribed value. This shows that the healthy state cannot be well described by means of the Mahalanobis distance when the frequencies are not normalized with respect to EOVs, which is most likely due to their non-Gaussian nature under perturbation by EOVs. It should be noted that without normalization the sensitivity to damages would probably be reduced drastically, besides the increased false alarms shown here.

On the other side, data normalization in Figure 10 (right) yields a false alarm rate under the envisaged 5% for each of the frequencies individually (except for one being right at the threshold), as well as for the combined evaluation of the frequencies, which emphasizes the need for data normalization to avoid false alarms.

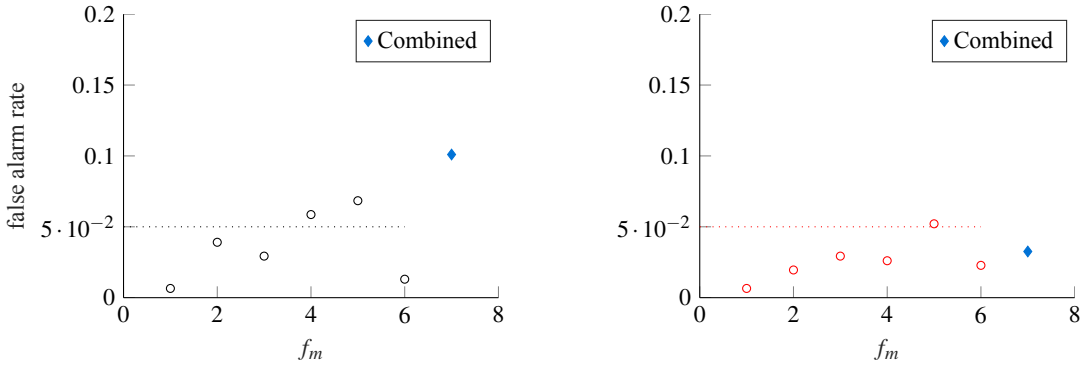

Fig. 10. False alarm rates on validation data without (left) and with data normalization (right), for the evaluation of each frequency individually as well as for their combined evaluation.

4 Conclusion

In this paper we have presented a framework for automated modal analysis and parameter tracking that is particularly robust to typical noisy conditions of ambient vibration testing, and combined it with a neural network-based approach for data normalization using measured EOVs. The framework has been applied to a case study on continuous monitoring of a footbridge, where the first six modes could be reliably identified and tracked throughout most of the datasets. The confounding variables have been shown to be the temperature and the energy of the vibration signals that are related to pedestrian load on the bridge. The subsequent data normalization based on these variables led to a significant reduction of the variability of the frequencies, and reduced false alarms when performing change detection.

Acknowledgements

The support from the ANR “France Relance” program is gratefully acknowledged.

References

1. C. Farrar, K. Worden, Structural health monitoring: A machine learning perspective, Wiley, Oxford, United Kingdom, 2012.
2. E. Reynders, J. Houbrechts, G. De Roeck, Fully automated (operational) modal analysis, Mechanical Systems and Signal Processing 29 (2012) 228–250.
3. V. Yaghoubi, M. K. Vakilzadeh, T. J. Abrahamsson, Automated modal parameter estimation using correlation analysis and bootstrap sampling, Mechanical Systems and Signal Processing 100 (2018) 289–310.
4. J. Priou, S. Greś, A. Mendler, M. Perrault, L. Guerineau, M. Döhler, Automated uncertainty-based clustering and tracking of modal parameters under strong variations, in: Proc. 10th International Operational Modal Analysis Conference (IOMAC), 2024.
5. E. Reynders, R. Pintelon, G. De Roeck, Uncertainty bounds on modal parameters obtained from stochastic subspace identification, Mechanical Systems and Signal Processing 22 (4) (2008) 948 – 969.
6. M. Döhler, L. Mevel, Efficient multi-order uncertainty computation for stochastic subspace identification, Mechanical Systems and Signal Processing 38 (2) (2013) 346–366.
7. S. Greś, R. Riva, C. Y. Süleyman, P. Andersen, M. Łuczak, Uncertainty quantification of modal parameter estimates obtained from subspace identification: An experimental validation on a laboratory test of a large-scale wind turbine blade, Engineering Structures 256 (2022) 114001.
8. A.-M. Yan, G. Kerschen, P. De Boe, J.-C. Golinval, Structural damage diagnosis under varying environmental conditions—part i: A linear analysis, Mechanical Systems and Signal Processing 19 (4) (2005) 847–864.
9. C. Rainieri, F. Magalhaes, D. Gargaro, G. Fabbrocino, A. Cunha, Predicting the variability of natural frequencies and its causes by second-order blind identification, Structural Health Monitoring 18 (2) (2019) 486–507.
10. E. Reynders, G. Wursten, G. De Roeck, Output-only structural health monitoring in changing environmental conditions by means of nonlinear system identification, Structural Health Monitoring 13 (2014) 82–93.
11. N. Dervilis, K. Worden, E. Cross, On robust regression analysis as a means of exploring environmental and operational conditions for shm data, Journal of Sound and Vibration 347 (2015) 279–296.
12. A. Cury, C. Cremona, J. Dumoulin, Long-term monitoring of a psc box girder bridge: Operational modal analysis, data normalization and structural modification assessment, Mechanical Systems and Signal Processing 33 (2012) 13–37.
13. L. D. Avendaño-Valencia, E. N. Chatzi, D. Tcherniak, Gaussian process models for mitigation of operational variability in the structural health monitoring of wind turbines, Mechanical Systems and Signal Processing 142 (2020) 106686.
14. B. Peeters, G. de Roeck, Reference-based stochastic subspace identification for output-only modal analysis, Mechanical Systems and Signal Processing 13 (6) (1999) 855 – 878.
15. M. Döhler, L. Mevel, Fast multi-order computation of system matrices in subspace-based system identification, Control Engineering Practice 20 (9) (2012) 882 – 894.
16. S. Greś, M. Döhler, Uncertainty propagation in subspace methods for operational modal analysis under misspecified model orders, in: Proc. 30th Conference on Noise and Vibration Engineering (ISMA), Leuven, Belgium, 2022.
17. M. Döhler, P. Andersen, L. Mevel, Variance computation of modal parameter estimates from UPC subspace identification, in: Proc. 7th International Operational Modal Analysis Conference (IOMAC), Ingolstadt, Germany, 2017.
18. J. Priou, A. Mendler, M. Perrault, L. Guerineau, M. Döhler, Normalization of environmental effects in modal parameter tracking, in: Proc. 10th International Operational Modal Analysis Conference (IOMAC), 2024.
19. Setra/AFGC, Technical guide – footbridges – assessment of vibrational behaviour of footbridges under pedestrian loading, Paris, France (2006).